

TETRADENTATE AZO SCHIFF BASE Ni(II), Pd(II) AND Pt(II) COMPLEXES: SYNTHESIS, SPECTRAL PROPERTIES, ANTIBACTERIAL ACTIVITY, CYTOTOXICITY AND DOCKING STUDIES

Hussein Abdulkadhim Hasan^{1*}, Saad M. Mahdi¹ and Hanaa Addai Ali²

¹Department of Chemistry, College of Science, University of Babylon, Babylon, Iraq

²Department Chemistry, College of Science, University of Kufa, Najaf, Iraq

(Received July 18, 2023; Revised October 16, 2023; Accepted October 19, 2023)

ABSTRACT. A new complexes of Ni(II), Pd(II), and Pt(II) have been synthesized from the reaction of Azo-Schiff base ligand (L1) that was prepared by the condensation firstly of salicylaldehyde with ethylene diamine in a 1:2 molar ratio and the prepared imine compound (S1) reacted with 2,5-dichloro aniline, and were employed in the preparation of complexes containing the metal ions Ni(II), Pd(II), and Pt(II). The structural characteristics of the synthesized compounds were investigated using UV-Vis, IR and NMR, molar conductance, elemental analysis, and mass spectroscopy. The results of the elemental analysis point to a 1:1 [M:L] stoichiometry. According to molar conductance studies, none of the prepared end products are electrolytic in nature. The complexes of Ni(II), Pd(II), and Pt(II) may have square planer geometry, according to spectral investigations. Then Pd(II), Ni(II), and Pt(II) complexes were evaluated for antimicrobial activity against different types strains of Gram-negative [*Escherichia coli* (ATCC 25922)] and positive bacteria [*Staphylococcus aureus* (ATCC 25923)] and showed good significant against these bacteria. The cytotoxic effect of the palladium complex on the prostatic malignant cell was examined via the PC3 cell line studied against normal cell WRL-68. The molecular docking of target microorganisms of these complexes will be studied by using MOE software.

KEY WORDS: Salen ligand, Nickel(II), Palladium(II), Platinum(II), Complexes, bis azo-Schiff base

INTRODUCTION

Coordination complexes have gained importance recently, particularly in the creation of long-acting drugs for metabolism. Owing to their biological and technological uses [1, 2] and applications in the augmentation of pharmacological action [3, 4]. Transition metals are important for usual functioning of living microorganisms and are, so, of great advantages as potential medications. The coordination chemistry of nitrogen atom donor ligands is an active area of research [5]. Research is being done on the coordination chemistry of nitrogen donor ligands. The complexes of metals with tetradentate ligands containing both oxygen and nitrogen have attracted a lot of attention in this field [6, 7]. A key group of ligands in coordination chemistry are the Schiff bases. For a better understanding of the intricate biological process, knowledge of the chemical makeup and binding characteristics of different Schiff base complexes may be crucial. Salicylaldehyde Schiff base-derived salen are well known for their intriguing ligational characteristics and unusual uses in a variety of industries [8–10]. According to the literature, the interaction between these donor ligands and metal ions may make these complexes more physiologically active. The popularity of Schiff bases and their metal complexes has grown recently due to their extensive biological activity [11, 12]. The above-mentioned fact and our earlier work on transition metal complexes with Schiff bases have both been taken into consideration while creating the ligand azo-Schiff base (L1) [13, 14]. In this study, the antibacterial activity of the ligand and its complexes with Ni(II), Pd(II), and Pt(II) were synthesized, characterized, and examined and the prostatic cancer cell line PC3 was examined for the palladium complex.

*Corresponding author. E-mail: huss17ein@gmail.com

This work is licensed under the Creative Commons Attribution 4.0 International License

EXPERIMENTAL

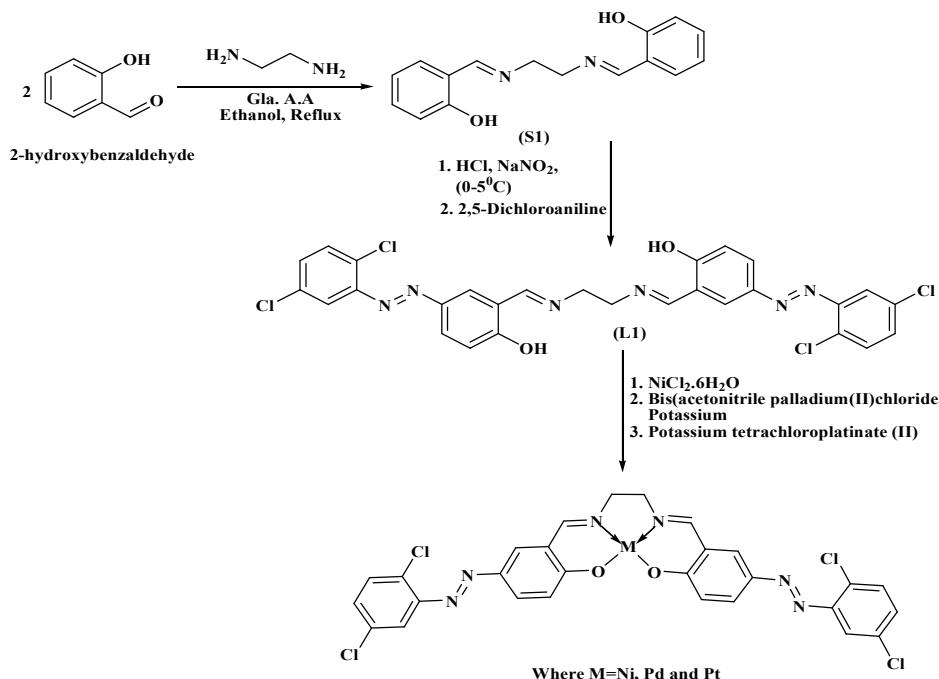
The analytical grade was employed for all research compounds and solvents, and they were used without additional purification. Salicylaldehyde, ethylenediamine, 2,5-dichloro aniline, NiCl₂, PdCl₂, and PtCl₂ were all bought from Aldrich, USA, and Merck directly. The methanol used for research was of spectroscopic quality. A PerkinElmer 2400 CHN Elemental Analyzer was used to conduct the elemental studies (C, H, and N). FTIR spectra were captured using the Bruker ALPHA FTIR (4000–400 cm⁻¹) and FTIR-ATR. TMS was used as an internal standard in the DMSO-*d*₆ solvent as it was used to gather ¹H and ¹³C NMR spectra on a Bruker 300 MHz and 75 MHz NMR spectrometer. On a Shimaduz spectrophotometer 1650PC model, UV-Visible spectra of the ligand and its complexes (200–1100 nm) were captured. Hanna model pH meters were used to record the pH measurements. Atomic absorption analysis using the Perkin-Elmer model 2280 was used to determine the complex's metal content. At room temperature, molar conductance in DMF (10⁻³ M) was measured using a conductivity meter and WTW InoLab Cond 720.

Synthesis of salen compound (S1)

The yellow-colored crystalline product was produced by dissolving ethylene diamine (10 mmol, 0.6 g, 0.67 mL) and salicylaldehyde (20 mmol, 2.44 g, 2.2 mL) in ethanol separately, mixing them together after adding three drops of glacial acetic acid, and then refluxing for an hour. The finished product was filtered, washed with ethanol, and then recrystallized with ethanol. The procured compound crystalline product was dried over anhydrous CaCl₂ under vacuum condition. Yield: 87%. M.F. (C₁₆H₁₆N₂O₂); colour: yellow; m.p. 126–128 °C; (TLC: ethylacetate:n-hexane 3:2, R_f: 0.81); FTIR data (cm⁻¹): 3405 (OH str.), 3050 (Ar-H), 2900, 2792 (C-H, sym., asym.), 1635 (C=N ring str.), 1577 (C=C ring str.), 1371 (C–N str.).

Synthesis of azo-Schiff ligand (L1) [15]

The azo Schiff ligand, referred to as L1, was synthesized by combining 2,5-dichloroaniline (5 mmol, 0.81 g) with 12 mL of hydrochloric acid (2 M) in a cooled environment. A solution of sodium nitrite (5 mmol, 0.33 g) dissolved in 5 mL of distilled water was slowly added drop by drop to the acidic solution of 2,5-dichloroaniline at a temperature between (0–5) °C. The resulting mixture was stirred for 30 min while maintaining the cooling conditions. The diazonium chloride solution of 2,5-dichloroaniline was slowly added drop by drop to a solution containing the previously synthesized imine compound (5 mmol, 1.34 g) dissolved in 10 mL of ethanol and 10 mL of 10% sodium hydroxide, while maintaining a cooled environment. The resulting reaction solution was allowed to sit overnight, resulting in the formation of a precipitate. The precipitated dye was then filtered, washed with water, and subsequently dried. Yield: 84%. colour: yellow; m.p: 132–134 °C; (TLC: ethylacetate:n-hexane 3:2, R_f: 0.65); cal (C₂₈H₂₀Cl₄N₆O₂); C 72.08%, N 14.10%, H 4.65%, found: C 72.01%, N 14.08%; H 4.44%; λ_{max} nm in DMSO 362 (π → π*) 284 (n → π*); FTIR data (cm⁻¹): 3412 (OH str.), 3090 (H–C=N ring str.), 2933 (Ar-H), 2890 (C–H, sym.), 1633 (C=N ring str.), 1590 (C=C ring str.), 1473 (N=N str.), 1385 (C–N str.), 1251 (C–O str.); ¹H NMR (300 MHz, DMSO-*d*₆): δ 13.47 (s, 2 H, OH), 8.41 (s, 2 H, NCH), 8.10–7.22 (m, 12H, Ar-H), 3.93 (s, 4 H, -CH₂), ¹³C NMR (75 MHz, DMSO-*d*₆): δ 166.74 (C of imine), 160.14 (OH-C of Ar), 145.84 (-N=N-C- of Ar ring), 142.79 (-N=N-C of Ar ring), 131.35, 130.07, 129.87, 127.91, 127.11, 124.74, 122.60, 121.12, 117.51 (18 C, Ar-C), 56.70 (-CH₂-N-).



Scheme 1. Synthesis azo-Schiff base complexes.

Synthesis of nickel(II) complex [16]

Complex was prepared as described in Scheme 1. A mixture of nickel(II) chloride hexahydrate (0.25 mmol, 0.032 g) was dissolved in mixture of methanol (10 mL), added dropwise to the ligand (L1) (0.5 mmol, 0.31 g) and dissolved in mixture of ethanol and chloroform (1:1, 40 mL). After the addition, the reaction solution's color changed to a dark brown. Overnight, the reaction mixture was refluxed for 24 hours. Using TLC with ethyl acetate:n-hexane as the mobile phase (1:4), the reaction was seen. At the conclusion of the reaction, just 30% of the reaction solution's total volume remained. Under vacuum, the solvent was extracted, and the residue was twice washed with hexane. Methanol was used to crystallize the resultant crystals.

Complex $[\text{Ni}(\text{C}_{28}\text{H}_{20}\text{Cl}_4\text{N}_6\text{O}_2)]$. m.p. 260-262 °C; yield, 84%; FTIR data (cm⁻¹): 3082 (Ar-H), 2929, 2827 (C-H, sym., asym.), 1618 (C=N str.), 1527 (C=C ring str.), 1377 (C-N str.), 1332 (C-O str.), 439 (Ni-N), 511 (Ni-O), ¹H NMR (300 MHz, DMSO-*d*₆): δ 8.67 (s, 2 H, NCH), 8.03-7.22 (m, 12H, Ar-H), 3.86 (s, 4 H, -CH₂).

Synthesis of palladium(II) complex [17]

Complex was set up in accordance with Scheme 2. Bis(acetonitrile)palladium dichloride was dissolved in acetonitrile (0.25 mmol, 0.065 g), added dropwise to the ligand (L1) (0.5 mmol, 0.31 g), and then dissolved in an ethanol and chloroform (1:1) combination in 40 mL. After the addition, the reaction solution's hue changed to brown. Overnight, the reaction mixture was refluxed for 24 hours. Using TLC with ethyl acetate:n-hexane as the mobile phase (1:4), the

reaction was seen. At the conclusion of the reaction, just 30% of the reaction solution's total volume remained. Under vacuum, the solvent was extracted, and the residue was twice washed with hexane. Brown powder was produced after the resultant solids crystallized from the methanol.

Complex [$Pd(C_{28}H_{20}Cl_4N_6O_2)$]. m.p. 271-273 °C; yield, 84%; FTIR data (cm^{-1}): 3083 (Ar-H), 2950, 2924 (C-H, sym., asym.), 1628 (C=N str.), 1594 (C=C ring str.), 1373 (C-N str.), 474 (Pd-N), 594 (Pd-O). 1H NMR (300 MHz, DMSO- d_6): δ 8.71 (s, 2 H, NCH), 7.99-7.25 (m, 12H, Ar-H), 3.85 (s, 4 H, -CH₂).

Synthesis of platinum(II) complexes [18]

A mixture of potassium tetrachloroplatinate(II), (0.25 mmol, 0.1 g) was dissolved in DMSO (5 mL), added dropwise to the mixture of ligand (L1) (0.5 mmol, 0.31 g) and sodium acetate (1 mmol) that dissolved in mixture of ethanol and chloroform (1:1, 40 mL), the pH of the reaction mixture fixed at 9.5. After the addition, the reaction solution's color changed to a dark brown. Overnight, the reaction mixture was refluxed for 24 hours. Using TLC with ethyl acetate:n-hexane as the mobile phase (1:4), the reaction was seen. At the conclusion of the reaction, just 30% of the reaction solution's total volume remained. Under vacuum, the solvent was extracted, and the residue was twice washed with hexane. The resultant solids from the methanol solidified to produce dark brown powder.

Complex [$Pt(C_{28}H_{20}Cl_4N_6O_2)$]. m.p. 137-139 °C; yield, 84%; FTIR data (cm^{-1}): 3084 (Ar-H), 2968, 2875 (C-H, sym., asym.), 1602 (C=N str.), 1514 (C=C ring str.), 1462 (C-N str.), 445 (Pt-N), 574 (Pt-O), 1H NMR (300 MHz, DMSO- d_6): δ 8.76 (s, 2 H, NCH), 8.06-7.23 (m, 12H, Ar-H), 3.83 (s, 4 H, -CH₂).

Antimicrobial bacterial cultures [19]

The antibacterial activity of the synthesized compounds was evaluated in vitro against two bacterial strains: *Staphylococcus aureus* (ATCC25923), a Gram-positive bacteria, and *Escherichia coli* (ATCC25922), a Gram-negative bacteria. The agar well diffusion method was employed to assess the activity. Serial dilutions in liquid broth were also carried out to determine the minimum inhibitory concentration (MIC) values of the compounds.

In vitro antimicrobial evaluation [20]

The synthesized compounds were subjected to the agar well diffusion assay using *Staphylococcus aureus* and *Escherichia coli* as test organisms. The microbial cultures were adjusted to a turbidity equivalent to a 0.5 McFarland turbidity standard and incubated at 37 °C. Mueller-Hinton agar plates were then swabbed uniformly with the standardized cultures and allowed to dry. Using a sterile cork-borer, three wells with a diameter of 6 mm were created on each plate, spaced approximately 2 cm apart. The bottom of each well was coated with sterilized Mueller-Hinton agar that was heated to 45 °C. The synthesized compound, dissolved in DMSO, was added to one of the wells, and allowed to diffuse at room temperature for 2 hours. The second well was loaded with DMSO as a negative control (-C), and the third well was loaded with streptomycin as a positive control (+C) for bacterial culture. All the plates were then incubated at 37 °C, with the agar surface facing upwards, among the bacterial cultures, for 24-48 hours. The diameter of the inhibition zone formed around each well was measured using a microscope scale, and five replications were performed for each plate.

Agar dilution method [21]

The determination of minimum inhibitory concentration (MIC) was carried out using the widely-used agar dilution method. This method involves the preparation of agar medium by incorporating different concentrations of the synthesized antimicrobial agent through serial twofold dilutions. A standardized microbial inoculum was then applied onto the surface of the agar plates. The MIC endpoint was determined as the lowest concentration of the antimicrobial agent that completely inhibited the growth of the microorganisms under appropriate incubation conditions. This technique is commonly employed for testing antibacterial susceptibility.

MTT protocol for cell line studied [22]

The cytotoxic effect of cuprizone 50 mM with presence different concentrations from levetiracetam was performed by using MTT ready to use kit (Intron Biotech):

A. Kit contents. MTT solution 1 mL x 10 vials. Solubilization solution 50 mL x 2 bottle.

B. Protocol. Tumor cells were cultured in 96 flat well micro-titer plates at concentrations ranging from 1×10^4 to 1×10^6 cells/mL. Each well was filled with 200 μ L of complete culture medium. The microplate was then covered with sterilized parafilm and gently shaken. The plates were incubated at 37 °C, 5% CO₂ for 24 h. Following the incubation period, the medium was aspirated, and the wells were subsequently treated with two-fold serial dilutions of levetiracetam at concentrations of 200, 100, 50, 10, 2.5, and 0.5 mM/mL. For each concentration, triplicates were prepared, including control samples where cells were treated with serum-free medium. The plates were then incubated at a temperature of 37 °C and a CO₂ concentration of 5% for a predetermined exposure time of 4 hours. 50 μ M/mL of cuprizone was added to each well for 24 H. After the exposure period, 10 μ L of MTT solution was added to each well, and the plates were incubated again at 37 °C with 5% CO₂ for 4 hours. Following this, the media were carefully removed, and 100 μ L of solubilization solution was added to each well for a duration of 5 min. The absorbance of the samples was then measured using an ELISA reader at a wavelength of 575 nm. The obtained optical density data were subjected to statistical analysis to calculate the concentration of the compounds that caused a 50% reduction in cell viability for each cell line. This calculation was performed using the provided equation: $Y = D + A \cdot D / (1 + 10^{(x - \log C) \cdot B})$.

RESULTS AND DISCUSSION

The trendy salen-type ligand (L1) was synthesized using the general method outlined in the provided references (Scheme 1) [23, 24]. The yield of these ligands obtained through this procedure was satisfactory, resulting in yellow amorphous powder. The synthesized compound exhibited good solubility in ethanol and was characterized using elemental analysis and spectroscopic techniques. The salen structure consists of two imine and two phenol moieties (L1), where the N₂O₂-imine chelating position is commonly observed in reference salen compounds (Scheme 1) [23]. While this chelating position's coordination chemistry has been extensively studied and mimicked [25, 26], the literature reveals that there are unique aspects of salen chemistry yet to be explored. In this research, we are investigating the antimicrobial activities of these trendy ligands for the first time. Additionally, IR/NMR, mass spectroscopy, and other relevant parameters have been included in this study. The exploration of the versatile chemistry of open-ended salen ligands represents an exciting research endeavor.

Molar conductance and elemental analysis

The spectral and analytical studies conducted on the compounds indicated that they possess stability and crystalline properties. The metal complexes showed good solubility in DMSO and DMF, whereas the ligand showed solubility in ethanol and acetone. The proposed structures corresponded well with the elemental analyses of the metal complexes and azo-Schiff base ligands. Furthermore, the complexes' low molar conductance values indicated that they are non-electrolytic in nature (Table 1).

Table 1. Analytical and physicochemical data of ligand and its metal complexes.

Compound	Elemental analysis (%): found (calc.)				m.p. °C	Color	Molar conductance $\Omega^{-1}\text{cm}^2 \text{mol}^{-1}$
	C	H	N	M			
L1	53.87 (54.75)	3.04 (3.28)	12.92 (13.68)	-	128- 130	Pale yellow	-
NiL1	49.75 (50.12)	2.45 (2.70)	12.10 (12.53)	7.97 (8.75)	260- 262	Brown	10.2
PdL1	46.84 (46.79)	2.31 (2.52)	11.14 (11.69)	13.98 (14.81)	271- 273	Brown	11.4
PtL1	42.37 (41.68)	2.10 (2.25)	10.05 (10.41)	23.87 (24.16)	130- 132	Yellow	8.3

FTIR data

The spectrum presents vital details concerning the functional groups attached to the metal center and their bonding characteristics. In the azo-Schiff base ligand (L1), a prominent peak at 1628 cm^{-1} corresponds to the stretching vibration of the (-C=N) group [27]. However, upon coordination in the prepared complexes, these vibrations shift to lower frequencies in the range of $1609\text{-}1618 \text{ cm}^{-1}$, indicating the chelation of the N atom from the imine group (-C=N) of the free ligand to the central metal ion [28]. In the ligand, a broadband appears at 3422 cm^{-1} , signifying the stretching vibration of the (-OH) group. In contrast, this band vanishes in the metal complexes, suggesting the deprotonation of the hydroxyl group and its involvement in coordination with the metal. This phenomenon can be attributed to the transfer of electrons from the N atom to the empty d-orbital of the metal atom. Moreover, two new bands emerge in the far-infrared region of the complexes, approximately around $588\text{-}511 \text{ cm}^{-1}$ and $474\text{-}438 \text{ cm}^{-1}$, which are assigned to the vibrations of $\nu(\text{M-O})$ and $\nu(\text{M-N})$, respectively. These bands provide evidence for the participation of the N atom from the (-C=N) group and the oxygen atom from the (-OH) group of the ligand in chelation.

Ultraviolet spectra and magnetic susceptibility measurement

The spectrum presented here is employed to differentiate between various geometries of the metal complexes. The ligand exhibits two absorption bands. The weak band observed at 362 nm is attributed to the $\pi \rightarrow \pi^*$ stacking interaction of the aromatic groups present in the Schiff base. Additionally, a strong band appears at 284 nm, which corresponds to the $n \rightarrow \pi^*$ transition of the C=N and N=N groups within the Schiff base. These bands undergo certain changes in the spectra of the complexes, indicating the coordination of the ligand to the metal center. The spectrum of Ni(II) complex shows one intensity band at 359 nm due to transfer intra ligand charge transfer transition (I.L.C.T.) and 409 nm, owing to due to metal to ligand charge transfer transition (M.L.C.T.) [29, 30]. The prepared Pd(II) complexes exhibit a broad d-d transition band around 490 nm, which is indicative of a metal-to-ligand charge transfer (M.L.C.T.) transition [31].

Additionally, a relatively strong charge transfer band is observed in the spectra of all the Pd(II) complexes at around 421 nm. Based on the electronic spectroscopic data and the diamagnetic behavior of the complexes, a square planar geometry is proposed for all the Pd(II) complexes. On the other hand, the Pt(II) complexes display diamagnetic properties and possess a low-spin d8 electronic configuration. Spin-allowed d-d transitions are observed at 403 nm, corresponding to a metal-to-ligand charge transfer (M.L.C.T.) transition, and at 302 nm, representing an intra-ligand charge transfer transition within the complexes. These transitions further confirm the square planar geometry of these Pt(II) complexes.

Magnetic susceptibility measurements are a valuable tool for characterizing the structures of metal complexes. The magnetic moment (μ) reflects the extent of paramagnetism in a compound, with a larger μ indicating a higher degree of paramagnetic behavior. The magnetic moment is influenced by both spin and orbital angular momentum. The presence of unpaired electrons in the partially filled d-orbitals of the outer shell of a compound contributes to its magnetic properties. In the case of the synthesized Ni(II) complex, the observed magnetic moment value indicates a diamagnetic character, as its moment approach to zero BM value [32]. This diamagnetic behavior is consistent with a square planar geometry for the Ni(II) complex. Similarly, the Pt(II) and Pd(II) complexes (PtL1 and PdL1) also exhibit diamagnetic properties. Therefore, these complexes are also likely to possess a square planar geometry, similar to the nickel complex.

NMR spectral studies

The ^1H NMR spectrum of the azo-Schiff base ligand (L1) and its complexes was recorded in a DMSO- d_6 solution. In the ligand spectrum, a group of signals appears as a multiplet in the range of 8.09-7.22 ppm, corresponding to the aromatic protons present in the compound [33]. Additionally, there is a peak at 13.47 ppm, which is assigned to the (-OH) protons in the ligand. However, in the spectra of the complexes, there is no distinct peak observed for the (-OH) group, indicating that the (-OH) protons have been deprotonated and a M-O bond has formed during the chelation process [34]. In the complexes' spectra, multiplet peaks are observed in the range of 8.06-7.22 ppm, which can be attributed to the aromatic protons. Apart from this change related to the (-OH) group, other signals in the complexes' spectra show minimal differences compared to the ligand spectrum.

Mass spectra

The mass spectrum of $[\text{Ni}(\text{C}_{28}\text{H}_{20}\text{Cl}_4\text{N}_6\text{O}_2)]$, $[\text{Pd}(\text{C}_{28}\text{H}_{20}\text{Cl}_4\text{N}_6\text{O}_2)]$ and $[\text{Pt}(\text{C}_{28}\text{H}_{20}\text{Cl}_4\text{N}_6\text{O}_2)]$ as shown in shows a molecular ion peak at m/z 670.11 due to $[\text{Ni}(\text{L1})]^+$, m/z 717.29 due to $[\text{Pd}(\text{L1})]^+$ and m/z 806.72 due to $[\text{Pt}(\text{L1})]^+$ which is consistent with the complexes' suggested formula.

Biological activity antimicrobial study

E. Coli MTCC 443 and *S. Aureus* MTCC 96 were the two bacteria against which the metal complexes were tested. The broth dilution method was used to assess antimicrobial activity. It was done with Mueller-Hinton agar nutrition media. Microbes were grown using the Hinton Broth Method, and the test's microbe compound suspension was diluted. In DMSO solvent (control), solutions of synthetic compounds were created. Overnight incubation at 37°C was also performed on the sample tubes. In order to investigate the antibacterial properties of the synthesized compounds, the minimum inhibitory concentration (MIC) for the control test microorganisms was noted.

Antimicrobial study

The antibacterial chemicals tested were effective against both gram-positive and gram-negative bacteria. Below are the steps taken for antibacterial investigations (Figure 1). Table 2 lists the mean zone diameter values for each drug as well as the MIC values for a few compounds. All of the chosen bacteria (*Staphylococcus aureus* and *Escherichia coli*) were responsive to the chemicals (NiL1, PdL1, and PtL1). Between the produced compounds, PtL1 was more effective against *Staphylococcus aureus* and against *Escherichia coli*.

Table 2. Antibacterial results of metal complexes.

Compound	Concentration $\mu\text{g/mL}$	<i>Escherichia coli</i>	<i>Staphylococcus aureus</i>
NiL1	100	14	34
	50	8	22
	25	5	18
	12.5	0	12
PdL1	100	13	19
	50	6	12
	25	2	7
	12.5	0	4
PtL1	100	16	36
	50	6	27
	25	3	20
	12.5	0	12

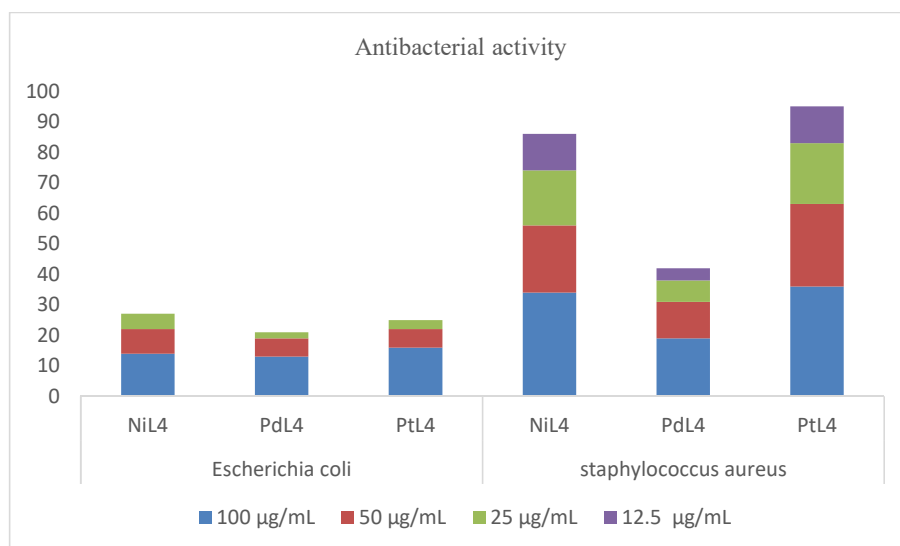


Figure 1. Antimicrobial activity of metal complexes (NiL1, PdL1, PtL1).

PC3 cell line study

The cytotoxicity of the palladium complex was examined toward the prostatic cancerogenic cells via the PC3 cell line study compared with normal cell line WRL-68 and the results was

demonstrated IC_{50} value (125.5) for the prostatic cancer cells compared with IC_{50} value (156.2) for the normal cell, these can be shown in Table 3 and Figure 2.

Table 3. The cytotoxic effect of Pd complex in PC3 cell line and normal WRL68 cell line.

Concentration $\mu\text{g mL}^{-1}$	Mean viability (%) \pm SD	
	WRL68	PC3
4 0 0	74.88 \pm 5.00	72.87 \pm 4.78
2 0 0	86.07 \pm 3.07	74.69 \pm 2.55
1 0 0	90.08 \pm 1.049	89.19 \pm 2.41
5 0	93.86 \pm 1.10	93.9 \pm 0.53
2 5	94.63 \pm 0.48	94.67 \pm 0.6

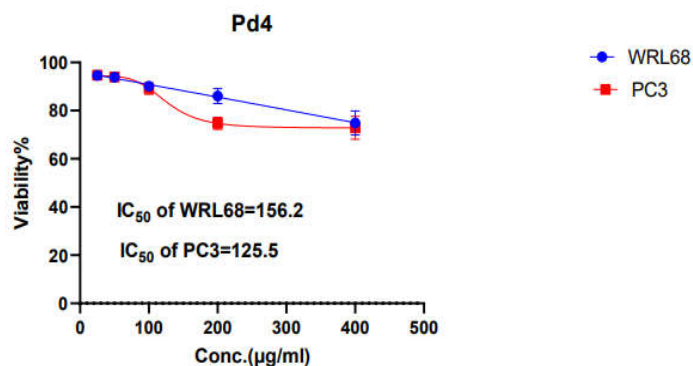


Figure 2. Anticancer data of the palladium complex.

Molecular docking

Molecular docking experiments were used in this investigation. The most important of many elements affecting the results against proteins to compare the activities of molecules is the chemical interaction between molecules and proteins in the study. In Figures 3 and 4 these chemical interactions are elaborately illustrated. Numerous parameters are calculated as a result of molecular docking calculations, which are done to compare the activities of the molecules and investigate the chemical interactions that take place. These computations include the computation of numerous parameters (Table 4). This table compares the activities of the compounds using some of the provided parameters, while others provide the numerical value of interactions between molecules and proteins (root mean square deviation (RMSD-refine), energy score (S), distance (S), and receptor).

Table 4. Docking interaction parameters for effective synthesized (NiL1, PdL1, PtL1) ligands against 1ecl and 4h8e proteins.

Protein	Compound docked	Receptor	Interactions	Distance (Å)	E (kcal/mol)	S (energy score)	rmsd_refine (Å)
1ecl	NiL1	Asp323 Ser 324	H-acceptor π -H	2.3 2.1	-1.2 -1.9	-6.0453	1.3636
1ecl	PdL1	Asn 555 Glu 487	H-doner H-doner	3.28 3.55	-0.3 -1.2	-7.0251	1.4725
1ecl	PtL1	Glu 579 Asp 576 Asp 562	H-doner H-doner Ione contact	3.60 3.47 2.60	-0.7 -1.4 -0.9	-5.6663	1.4929
4h8e	NiL1	Asn 81 Ser 209 Ser 209	H-acceptor π -H π -H	3.34 3.87 3.91	-3 -0.9 -0.7	-6.8534	1.3564
4h8e	PdL1	Thr 120	π -H	4.66	-0.6	-6.0003	1.3701
4h8e	PtL1	Phe 221 Ser 217	H- π π -H	4.07 4.03	-0.7 -0.8	-6.5929	1.6341

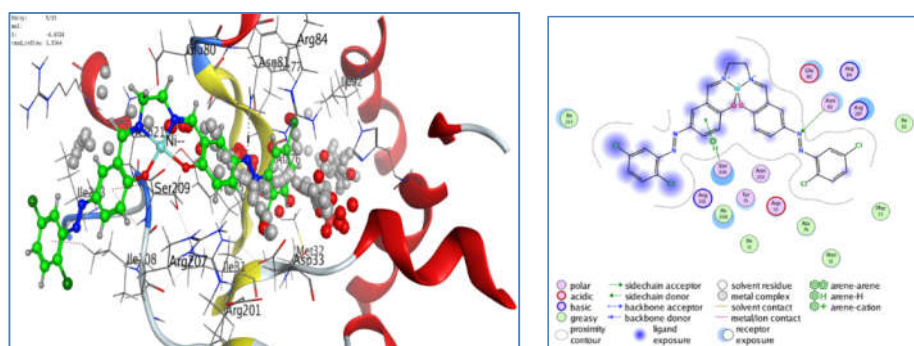


Figure 3. Diagrams depicting the docked conformation of ligands (NiL1) against 4h8e in 2D and 3D.

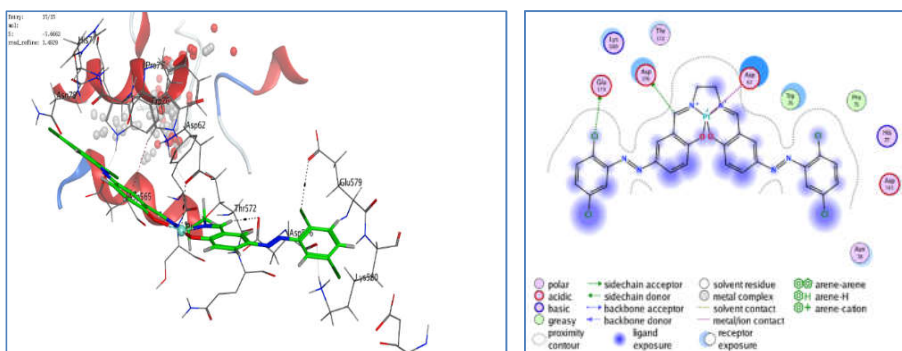


Figure 4. Diagrams depicting the docked conformation of ligands (PtL1) against 1ecl in 2D and 3D.

The other variables, on the other hand, are linked to exposure as a result of chemical interactions between chemicals and proteins. The following is how the docking experiments, in this case, explain the bond distances: When the interaction between NiL1 and 4h8e protein is studied, side chain acceptor (H-acceptor) interaction occurs with Asn 81 protein at 3.34 Å distances in azo group of ligand (Figure 3) Presentation of interactions of complexes), the interactions were (π -H) interaction occurs with Ser209 protein at 3.87, 3.91 Å distances with 4h8e protein. On the other hand, PdL4 is observed to form hydrogen bonds from the Thr 120 protein through the (π -H) interaction at 4.66 Å. On the other hand, the Phe 221 protein and PtL4 engage via (H- π) interactions at distances of 4.7 Å and observed (π -H) interaction from the Ser 217 protein at 4.03 Å. Where the docking score was (-6.8534, -6.0003, -6.5929) in addition to the root mean square deviation between the pose before refinement and the pose after refinement was (1.3564, 1.3701, 1.6341) respectively. In Figure 4, presentation of interactions of (NiL1, PdL1, PtL1) with 1ecl protein, when the interaction between NiL1 and 1ecl protein is examined, it is seen that metal ion interaction with the LYS244 protein at 3.1 Å. The (Cl) atom that attached the aromatic ring backbone acceptor interacted with the ASP409 proteins at 3.40 Å. The aromatic ring attached with chloro atoms forms an arene-cation (π -cation) interaction with the ARG430 protein at 3.76 Å and arene-H (π -H) interaction with the ILe428 protein at 4.60 Å. The docking scores of prepared complexes were (-6.5478, -7.4728, -6.4278) in addition to the root mean square deviation between the pose before refinement and the pose after refinement was (1.44458, 1.0127, 0.9136), respectively.

CONCLUSION

In this investigation, a novel Schiff base ligand and its complexes were synthesized through a non-template method. The obtained analytical data suggest that these complexes possess a mononuclear structure with one metal ion per molecule. Based on the magnetic moment values and electronic spectroscopic data, the Pd(II) and Pt(II) metal complexes adopt square planar structure, while the Ni(II) complex favors a tetrahedral structure. The synthesized ligands and metal complexes were assessed for their antibacterial activity against both Gram-positive and Gram-negative bacteria using the Minimum Inhibitory Concentration (MIC) method. Among the tested compounds, the Pt(II) complexes displayed the most potent antibacterial activity against all the tested strains, surpassing both standard drugs and other metal complexes in terms of efficacy.

REFERENCES

1. Shibuya, Y.; Nabari, K.; Kondo, M.; Yasue, S.; Maeda, K.; Uchida, F.; Kawaguchi, H. The copper(II) complex with two didentate schiff base ligands. The unique rearrangement that proceeds under alcohol vapor in the solid state to construct noninclusion structure. *Chem. Lett.* **2008**, *37*, 78-79.
2. Gangani, B.J.; Parsania, P.H. Microwave-irradiated and classical syntheses of symmetric double Schiff bases of 1,1'-bis (4-aminophenyl) cyclohexane and their physicochemical characterization. *Spectrosc. Lett.* **2007**, *40*, 97-112.
3. Kumari, B.S.; Rijulal, G.; Mohanan, K. Microwave assisted synthesis, spectroscopic, thermal and biological studies of some lanthanide(III) chloride complexes with a heterocyclic Schiff base. *Synth. React. Inorg. Met.-Org. Nano-Met. Chem.* **2009**, *39*, 24-30.
4. Thankamony, M.; Mohanan, K. Synthesis, spectral studies, thermal decomposition kinetics, reactivity and antibacterial activity of some lanthanide(III) nitrate complexes of 2-(N-indole-2-one)amino-3-carboxyethyl-4,5,6,7-tetrahydrobenzo [b] thiophene. *Indian J. Chem.* **2007**, *46A*, 247-251.

5. Raman, N.; Dhaveethu Raja, J.; Sakthivel, A. Synthesis, spectral characterization of Schiff base transition metal complexes: DNA cleavage and antimicrobial activity studies. *J. Chem. Sci.* **2007**, *119*, 303-310.
6. Halli, M.B.; Patil, V.B. Synthesis, spectral characterization and DNA cleavage studies of Co(II), Ni(II), Cu(II), Zn(II), Cd(II) and Hg(II) complexes with benzofuran-2-carbohydrazide Schiff bases. *Ind. J. Chem.* **2011**, *50A*, 664-669.
7. Shashidhar; Shivakumar, K.; Halli, M.B. Synthesis, characterization and antimicrobial studies on metal complexes with a naphthofuran thiosemicarbazide derivatives. *J. Coord Chem*, **2006**, *59*, 1847-1856.
8. Bharti, N.; Sharma, S.; Naqvi, F.; Azam, A. New palladium(II) complexes of 5-nitrothiophene-2-carboxaldehyde thiosemicarbazones: Synthesis, spectral studies and in vitro anti-amoebic activity. *Bioorg. Med. Chem.* **2003**, *11*, 2923-2929.
9. Soliman, A.A. Synthesis and properties of new substituted 1,2,4-triazoles: Potential antitumor agents. *J. Therm. Anal. Calorim.* **2001**, *63*, 221.
10. Dharmaraj, N.; Viswanathamurthi, P.; Natarajan, K. Ruthenium(II) complexes containing bidentate Schiff bases and their antifungal activity. *Transit. Met. Chem.* **2001**, *26*, 105-109.
11. Habila, A.N.P.; Naomi, P.N.; Hauwa, S.B.; Grema, M.; Adekunle, A.O.; Hussaini, G. Synthesis, characterization and antimicrobial analysis of Schiff bases of *o*-phenylenediamine and 2-aminopyridine-3-carboxylic acid with ofloxacin and their metal(II) complexes. *Bull. Chem. Soc. Ethiop.* **2020**, *14*, 263-278.
12. Heshmatpour, F.; Ghassemzadeh, M.; Bahemmat, S.; Malakootikhah, J.; Neumüller, B.; Rothenberger, A. Synthesis, characterization and molecular structure of a new tetrameric palladium(II) complex containing Schiff-bases derived from AMTTO (AMTTO = 4-amino-6-methyl-1,2,4-triazine-thione-5-one). *Z. Anorg. Allg. Chem.* **2007**, *633*, 1178-1182.
13. Mobinikhaledi, A.; Forughifar, N.; Kalhor, M. Synthesis, characterization, DNA binding and nuclease activity of binuclear copper(II) complexes of cuminaldehydethiosemicarbazones. *Turk. J. Chem.* **2010**, *34*, 367-373.
14. Illán-Cabeza, N.A.; Vilaplana, R.A.; Alvarez, Y.; Akdi, K.; Kamah, S.; Hueso-Ureña, F.; Quirós, M.; González-Vílchez, F.; Moreno-Carretero, M.N. Synthesis, structure and biological activity of a new and efficient Cd(II)-uracil derivative complex system for cleavage of DNAJ. *Biol. Inorg. Chem.* **2005**, *10*, 924-934.
15. Abbas, G.J.; Mosaa, Z.; Radhi, A.J.; Abbas, H.K.; Najem, W.M. Synthesis, studying analytical properties and biological activity of new transition metal complexes with sulfadiazine derivative as reagent. *Egypt. J. Chem.* **2023**, *66*, 55-61.
16. Jailani, A.K.; Gowthaman, N.S.K.; Kesavan, M.P. Synthesis, characterisation and biological evaluation of tyramine derived schiff base ligand and its transition metal(II) complexes. *Kar. Int. J. Mod. Sci.* **2020**, *6*, 15.
17. Balinge, K.R.; Bhagat, P.R. A polymer-supported salen-palladium complex as a heterogeneous catalyst for the Mizoroki-Heck cross-coupling reaction. *Inorgan. Chim. Acta* **2019**, *495*, 119017.
18. Hashemi, M.; Solati, Z.; Ghodsi, A.; Ahmadian, S. Azo-substituted Schiff base complex of Pt(II): Synthesis, characterization, DFT and TD-DFT study. *Synth. Met.* **2015**, *210*, 398-403.
19. Raj, J.; Jain, A.; Sharma, N.; Kumari, A.; Fahmi, N. Synthesis, spectral characterization, and biological activities of novel palladium(II) and platinum(II) complexes of active Schiff base ligands. *Bull. Chem. Soc. Ethiop.* **2023**, *37*, 1383-1396.
20. Radhi, E.R.; Ali, F.J.; Ali, K.J. Synthesis and characterization of a new azo quinoline ligand and its metal complexes with spectrophotometric determination and biological efficacy study of its Hg(II) complex. *Bull. Chem. Soc. Ethiop.* **2023**, *37*, 1423-1433.
21. Radhi, A.J.; Zimam, E.H.; Jafer, E.A. New barbiturate derivatives as potent in vitro α -glucosidase inhibitors. *Egypt. J. Chem.* **2021**, *64*, 117-123.

22. Abu-Yamin, A.A.; Abduh, M.S.; Saghir, S.A.M., Al-Gabri, N. Synthesis, characterization and biological activities of new Schiff base compound and its lanthanide complexes. *Pharm.* **2022**, *15*, 454.
23. Kargar, H.; Fallah-Mehrjardi, M.; Behjatmanesh-Ardakani, R.; Rudbari, H.A.; Ardakani, A.A.; Sedighi-Khavidak, S.; Munawar, K.S.; Ashfaq, M.; Tahir, M.N. Binuclear Zn(II) Schiff base complexes: Synthesis, spectral characterization, theoretical studies and antimicrobial investigations. *Inorg. Chim. Acta* **2022**, *530*, 120677.
24. Das, L.K.; Biswas, A.; Frontera, A.; Ghosh, A. Polymorphism in hetero-metallic tri-nuclear CuII2CdII complexes of salicylaldimine ligand: Structural analysis and theoretical study. *Polyhedron* **2013**, *52*, 1416-1424.
25. Majumdar, D.; Tüzün, B.; Pal, T. K.; Das, S.; Bankura, K. Architectural view of flexible aliphatic-OH group coordinated hemi-directed Pb(II)-Salen coordination polymer: synthesis, crystal structure, spectroscopic insights, supramolecular topographies, and DFT perspective. *J. Inorg. Organomet. Polym. Mater.* **2022**, *32*, 1159-1176.
26. Dolai, M.; Mistri, T.; Panja, A.; Ali, M. Diversity in supramolecular self-assembly through hydrogen-bonding interactions of non-coordinated aliphatic-OH group in a series of heterodinuclear CuIIM (M = NaI, ZnII, HgII, SmIII, BiIII, PbII and CdII). *Inorg. Chim. Acta* **2013**, *399*, 95-104.
27. Obaid, E.K.; Shaheed, H.A.; Najlaa, N.; Ahmed, K.H.; Mubarak, A.S.; Radhi, A.J. Synthesis and design of new gemcitabine derivatives as in vitro α -glucosidase inhibitors. *JGPT* **2009**, *11*, 25-29.
28. Burlov, A.S.; Vlasenko, V.G.; Koshchienko, Y.V.; Makarova, N.I.; Zubenko, A.A.; Drobin, Y.D.; Garnovskii, D.A. Synthesis, characterization, luminescent properties and biological activities of zinc complexes with bidentate azomethine Schiff-base ligands. *Polyhedron* **2018**, *154*, 65-76.
29. Sorrell, T.N.; O'Connor, C.; Anderson, O.P.; Reibenspies, J.H. Synthesis and characterization of phenolate-bridge copper dimers with a copper-copper separation of > 3.5 Å. Models for the active site of oxidized hemocyanin derivatives. *J. Am. Chem. Soc.* **1985**, *107*, 4199-4206.
30. Iskander, M.F.; El-Sayed, L.; Salem, N.M.; Werner, R.; Haase, W. Synthesis, characterization and magnetochemical studies of dicopper(II) complexes derived from bis (N-salicylidene) dicarboxylic acid dihydrazides. *J. Coord. Chem.* **2005**, *58*, 125-139.
31. Shanker, K.; Reddy, P.M.; Rohini, R.; Ho, Y.P.; Ravinder, V. Encapsulation of Pd(II) by N4 and N2O2 macrocyclic ligands: their use in catalysis and biology. *J. Coord. Chem.* **2009**, *62*, 3040-3049.
32. Sobha, S.; Mahalakshmi, R.; Raman, N. Studies on DNA binding behaviour of biologically active transition metal complexes of new tetradentate N2O2 donor Schiff bases: Inhibitory activity against bacteria. *Spectrochim. Acta Part A: Mol. Biomol.* **2012**, *92*, 175-183.
33. Hussein, A.A.; Albarazanchi, S.I.; AL-Shanon, A.F. Evaluation of anticancer potential for L-glutaminase purified from *Bacillus subtilis*. *Int. J. Pharm. Res.* **2020**, *12*, 123-128.
34. Hoonur, R.S.; Patil, B.R.; Badiger, D.S.; Vadavi, R.S.; Gudasi, K.B.; Dandawate, P.R.; Ghaisas, M.M.; Padhye, S.B.; Nethaji, M. Transition metal complexes of 3-aryl-2-substituted 1,2-dihydroquinazolin-4 (3H)-one derivatives: New class of analgesic and anti-inflammatory agents. *Eur. J. Med. Chem.* **2010**, *45*, 2277-2282.